

SDSS J080531.84+481233.0: AN UNRESOLVED L DWARF/T DWARF BINARY

ADAM J. BURGASSER¹

Massachusetts Institute of Technology, Kavli Institute for Astrophysics and Space Research, Building 37,
Room 664B, 77 Massachusetts Avenue, Cambridge, MA 02139, USA; ajb@mit.edu

Received 2007 March 23; accepted 2007 June 12

ABSTRACT

SDSS J080531.84+481233.0 is a peculiar L-type dwarf that exhibits unusually blue near-infrared and mid-infrared colors and divergent optical (L4) and near-infrared (L9.5) spectral classifications. These peculiar spectral traits have been variously attributed to condensate cloud effects or subsolar metallicity. Here I present an improved near-infrared spectrum of this source which further demonstrates the presence of weak CH₄ absorption at 1.6 μm but no corresponding band at 2.2 μm . It is shown that these features can be collectively reproduced by the combined light spectrum of a binary with L4.5 and T5 components, as deduced by spectral template matching. Thus, SDSS J080531.84+481233.0 appears to be a new low-mass binary straddling the L dwarf/T dwarf transition, an evolutionary phase for brown dwarfs that remains poorly understood by current theoretical models. The case of SDSS J080531.84+481233.0 further illustrates how a select range of L dwarf/T dwarf binaries could be identified and characterized without the need for high angular resolution imaging or radial velocity monitoring, potentially alleviating some of the detection biases and limitations inherent to such techniques.

Key words: binaries: general — stars: fundamental parameters —
stars: individual (SDSS J080531.84+481233.0) — stars: low-mass, brown dwarfs

Online material: color figures

1. INTRODUCTION

Coeval systems, from binaries to dense clusters, are invaluable resources for stellar studies. By significantly reducing uncertainties in distance, age, and composition, multiple systems enable comparative analyses of atmospheric properties, circumstellar environments, magnetic activity trends, and angular momentum evolution. Close binary systems also facilitate dynamical mass measurements, as well as radius measurements for eclipsing systems. The multiplicity characteristics of a coeval population provide critical constraints for theories exploring stellar genesis, as well as the distribution of stellar and substellar masses and the incidence of planetary systems throughout the Galaxy.

Multiple systems are of particular importance in studies of the lowest-mass stars incapable of sustained core hydrogen fusion, the so-called brown dwarfs. The apparently low resolved binary fraction of field brown dwarfs ($\sim 10\%–15\%$; see Burgasser et al. 2007b and references therein) has been cited as evidence of mass-dependent multiple formation (e.g., Bouy et al. 2006), as predicted by some brown dwarf formation models (e.g., Sterzik & Durisen 2003). However, resolved imaging studies provide only a lower limit to the true binary fraction, and evidence from radial velocity studies (e.g., Maxted & Jeffries 2005) and overluminous cluster members (Pinfield et al. 2003; Chappelle et al. 2005; Bouy et al. 2006) suggests a much higher total binary fraction, perhaps 25% or more (Basri & Reiners 2006; Reid et al. 2006). This may prove to be a significant challenge for some brown dwarf formation theories (e.g., Bate et al. 2002).

Unresolved multiples also play an important role in understanding the transition between the two lowest luminosity classes of known brown dwarfs, the L dwarfs and T dwarfs (Kirkpatrick 2005 and references therein). This transition occurs when pho-

spheric condensates, a dominant source of opacity in L dwarf atmospheres, disappear, resulting in near-infrared spectral energy distributions that are blue and dominated by molecular gas absorption, including CH₄ (Tsuji et al. 1996, 1999; Burrows & Sharp 1999; Chabrier et al. 2000; Allard et al. 2001). While condensate cloud models provide a physical basis for this transition (Ackerman & Marley 2001; Cooper et al. 2003; Burrows et al. 2006), they fail to explain its apparent rapidity, as deduced by the small effective temperature (T_{eff}) differential (Kirkpatrick et al. 2000; Golimowski et al. 2004; Vrba et al. 2004) and apparent brightening at 1 μm (Dahn et al. 2002; Tinney et al. 2003; Vrba et al. 2004) between late-type L dwarfs and midtype T dwarfs. Multiplicity effects may be partly responsible for these trends, particularly as the resolved binary fraction of L/T transition objects is nearly twice that of other spectral types (Burgasser et al. 2006), and can result in overestimated temperatures and surface fluxes (Golimowski et al. 2004; Liu et al. 2006). As the total binary fraction of L/T transition objects may be higher still (perhaps as high as 65%; Burgasser 2007), interpretations of absolute brightness, color, and T_{eff} trends across this important evolutionary phase for nearly all brown dwarfs may be skewed.

Empirical constraints on the L/T transition can be made through the identification and characterization of binaries with components that span this transition (Cruz et al. 2004; Burgasser et al. 2005, 2006; Liu et al. 2006; Reid et al. 2006). One such system that may have been overlooked is the peculiar L dwarf SDSS J080531.84+481233.0 (hereafter SDSS J0805+4812; Hawley et al. 2002; Knapp et al. 2004), identified in the Sloan Digital Sky Survey (hereafter SDSS; York et al. 2000). This source has widely discrepant optical (L4; Hawley et al. 2002) and near-infrared ($L9.5 \pm 1.5$; Knapp et al. 2004; Chiu et al. 2006) spectral types, and unusually blue near-infrared colors ($J - K = 1.10 \pm 0.04$; Knapp et al. 2004) compared to either L4 ($\langle J - K \rangle = 1.52$) or L8–T0.5 dwarfs ($\langle J - K \rangle = 1.58–1.74$; Vrba et al. 2004). Its mid-infrared colors are also peculiar (Golimowski et al. 2004; Knapp et al. 2004; Leggett et al. 2007). These characteristics

¹ Visiting Astronomer at the Infrared Telescope Facility, which is operated by the University of Hawaii under cooperative agreement NCC5-538 with the National Aeronautics and Space Administration, Office of Space Science, Planetary Astronomy Program.

have been interpreted as resulting from a metal-poor photosphere or one with unusually thin photospheric condensate clouds (Knapp et al. 2004; Golimowski et al. 2004; Leggett et al. 2007; Folkes et al. 2007). However, unresolved multiplicity may provide a better explanation for the peculiar properties of this source. In this article I present and analyze new low-resolution near-infrared spectral data for SDSS J0805+4812 that support this hypothesis, and demonstrate that this source is likely to be a binary with components straddling the L/T transition. Spectral observations are described in § 2, including a detailed discussion of the unusual features observed in these data. Analysis of these data in regard to the source's possible binary nature is described in § 3, and the properties of the components inferred from this analysis are discussed in § 4. Finally, the implications of this study, including application of the technique used here to identify and characterize brown dwarf binaries independent of angular resolution limitations, are briefly discussed in § 5.

2. OBSERVATIONS

2.1. Data Acquisition and Reduction

Low-resolution near-infrared spectral data for SDSS J0805+4812 were obtained on 2006 December 24 (UT) using the SpeX spectrograph (Rayner et al. 2003) mounted on the 3 m NASA Infrared Telescope Facility (IRTF). The conditions were clear with good seeing ($0.8''$ at J band). The $0.5''$ slit was employed, providing $0.75\text{--}2.5\ \mu\text{m}$ spectroscopy with a resolution of $\lambda/\Delta\lambda \approx 120$ and dispersion across the chip of $20\text{--}30\ \text{\AA}\ \text{pixel}^{-1}$. To mitigate the effects of differential refraction, the slit was aligned to the parallactic angle. Six exposures of 120 s each were obtained in an ABBA dither pattern along the slit. The A0 V star HD 71906 was observed immediately afterward at a similar air mass ($z = 1.18$) for flux calibration. Internal flat field and argon arc lamps were also observed for pixel response and wavelength calibration.

Data were reduced using the SpeXtool package, version 3.4 (Cushing et al. 2004), using standard settings. Raw science images were first corrected for linearity, pairwise subtracted, and divided by the corresponding median-combined flat-field image. Spectra were optimally extracted using the default settings for aperture and background source regions, and wavelength calibration was determined from arc lamp and sky emission lines. The multiple spectral observations were then median-combined after scaling individual spectra to match the highest signal-to-noise ratio observation. Telluric and instrumental response corrections for the science data were determined using the method outlined in Vacca et al. (2003), with line-shape kernels derived from the arc lines. Adjustments were made to the telluric spectra to compensate for differing H I line strengths in the observed A0 V spectrum and pseudovelocity shifts. Final calibration was made by multiplying the spectrum of SDSS J0805+4812 by the telluric correction spectrum, which includes instrumental response correction through the ratio of the observed A0 V spectrum to a scaled, shifted, and deconvolved Kurucz² model spectrum of Vega.

2.2. The Spectrum of SDSS J0805+4812

The reduced spectrum of SDSS J0805+4812 is shown in Figure 1 and compared to equivalent SpeX prism data for the optically classified L4 2MASS J11040127+1959217 (hereafter 2MASS J1104+1959; Cruz et al. 2003), and 2MASS J03105986+1648155 (hereafter 2MASS J0310+1648; Kirkpatrick et al. 2000), which is classified as L8 in the optical and L9 in the near-infrared (Geballe et al. 2002). The spectrum of SDSS J0805+4812 is most similar to

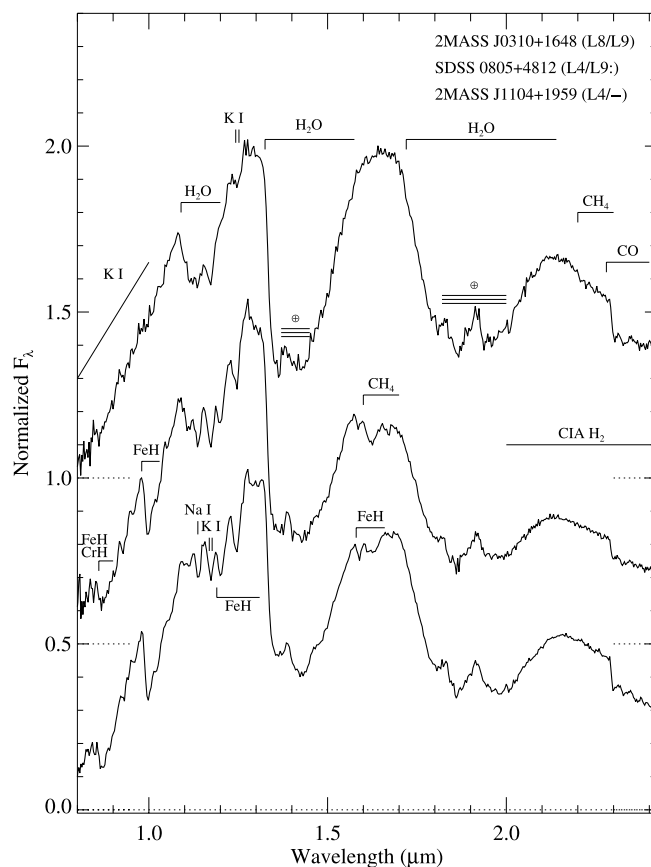


FIG. 1.— Reduced SpeX prism spectrum for SDSS J0805+4812 (middle) compared to equivalent data for the optically classified L4 2MASS J1104+1959 (bottom) and the L8/L9 (optical/near-infrared type) 2MASS J0310+1648 (top). All three spectra are normalized at their $1.25\ \mu\text{m}$ flux peaks and offset by constants (dotted lines). Prominent features resolved by these spectra are indicated. Note in particular the weak band of CH_4 at $1.6\ \mu\text{m}$ in the spectrum of SDSS J0805+4812.

that of 2MASS J1104+1959 based on their overall spectral energy distributions, strong FeH absorption at $0.99\ \mu\text{m}$, and prominent Na I and K I lines in the $1.1\text{--}1.25\ \mu\text{m}$ range. However, the 1.15 and $1.3\ \mu\text{m}$ H_2O bands are clearly much stronger in the spectrum of SDSS J0805+4812 but similar in strength to those in the spectrum of 2MASS J0310+1648. Other spectral characteristics of SDSS J0805+4812 are inconsistent with either of the comparison sources, such as the suppressed K -band flux peak and weak CO absorption at $2.3\ \mu\text{m}$.

The most unusual feature observed in the spectrum of this source, however, is the distinct absorption band at $1.6\ \mu\text{m}$, which is offset from $1.55\text{--}1.6\ \mu\text{m}$ FeH absorption seen in the spectra of 2MASS J1104+1959 (Fig. 1) and other midtype L dwarfs (Cushing et al. 2003). The $1.6\ \mu\text{m}$ feature is instead coincident with the Q -branch of the $2\nu_3$ CH_4 band, a defining feature for the T dwarf spectral class. It should be noted that this feature appears to be weakly present but overlooked in spectral data from Knapp et al. (2004), and no mention is made of it by Chiu et al. (2006), who also obtained SpeX prism data for SDSS J0805+4812. Interestingly, there is no indication of the $2.2\ \mu\text{m}$ CH_4 band, which is commonly seen in the spectra of the latest-type L dwarfs (this band is weakly present in the spectrum of L8/L9 2MASS J0310+1648; Fig. 1).

Several of the peculiar spectral characteristics of SDSS J0805+4812 are similar to those shared by a subclass of so-called blue L dwarfs (Cruz et al. 2003, 2007; Knapp et al. 2004; Burgasser et al. 2007a), including the blue spectral energy distribution, strong H_2O absorption, and weak CO bands. These properties can be explained

² See <http://kurucz.harvard.edu/stars.html>.

by the presence of thinner photospheric condensate clouds (Burgasser et al. 2007a), which enhances the relative opacity of atomic and molecular species around $1 \mu\text{m}$ and produces bluer $J - K$ and mid-infrared colors (Marley et al. 2002; Knapp et al. 2004; Leggett et al. 2007). However, Golimowski et al. (2004) have found that the thin cloud interpretation fails to explain the unusually blue $K - L'$ colors of SDSS J0805+4812, nor does it explain the presence of CH_4 absorption at $1.6 \mu\text{m}$ but not at $2.2 \mu\text{m}$. Subsolar metallicity has also been cited as an explanation for the peculiar nature of SDSS J0805+4812 (Golimowski et al. 2004; Knapp et al. 2004), although this source does not show the extreme peculiarities observed in the spectra of L subdwarfs (Burgasser et al. 2003b), nor does subsolar metallicity explain the presence of CH_4 absorption.

A potential clue to the nature of SDSS J0805+4812 can be found by noting that only two other late-type dwarfs have CH_4 absorption at $1.6 \mu\text{m}$ but not at $2.2 \mu\text{m}$: 2MASS J05185995–2828372 (hereafter 2MASS J0518–2828; Cruz et al. 2004) and SDSS J141530.05+572428.7 (Chiu et al. 2006). The latter source has not been studied in detail, but in the case of 2MASS J0518–2828 Cruz et al. (2004) have found that the combined light spectrum of an L6 plus T4 binary provides a reasonable match to the near-infrared spectrum of this source, including its weak CH_4 band. Subsequent high-resolution imaging has resolved this source into two point-source components and apparently confirms this hypothesis (Burgasser et al. 2006). The similarity in the spectral peculiarities between 2MASS J0518–2828 and SDSS J0805+4812 suggests that the latter may be a similar but as yet unrecognized pair.

3. BINARY TEMPLATE MATCHING

To explore the binary hypothesis for SDSS J0805+4812, the technique of binary spectral template matching was employed.³ A large set of binary spectral templates was constructed from a sample of 50 L and T dwarf SpeX prism spectra, including sources that are unresolved in high angular resolution imaging,⁴ and are not reported as spectrally peculiar. The individual spectra were flux-calibrated using the M_K –spectral type relation of Burgasser (2007) based on published optical and near-infrared spectral types for L dwarfs and T dwarfs, respectively, and synthetic MKO⁵ magnitudes determined directly from the spectra. Binaries were then constructed by combining spectral pairs with types differing by 0.5 subclasses or more, resulting in 1164 unique templates. Then χ^2 deviations⁶ were computed between the spectra of the synthesized binaries and SDSS J0805+4812 over the 1.0 – 1.35 , 1.45 – 1.8 , and 2.0 – $2.35 \mu\text{m}$ regions (i.e., avoiding regions of strong telluric absorption) after normalizing at $1.25 \mu\text{m}$. The single L and T dwarf spectra were also compared to that of SDSS J0805+4812 in a similar manner.

The best-match binary template for SDSS J0805+4812 is shown in Figure 2, composed of the L5 2MASS J15074769–1627386 (hereafter 2MASS J1507–1627; Reid et al. 2000) and the T5.5 2MASS J15462718–3325111 (hereafter 2MASS J1546–3325;

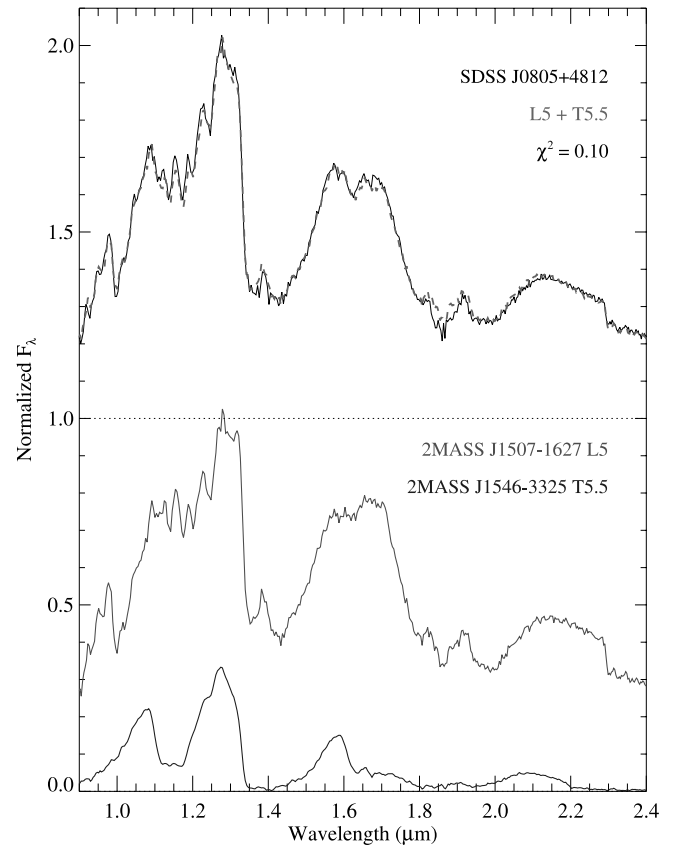


FIG. 2.— Best-match binary spectral template for SDSS J0805+4812, a combination of the L5 2MASS J1507–1627 and the T5.5 2MASS J1546–3325, shown in the bottom panel (gray and black lines, respectively). The combined spectrum (top, dashed line) is an excellent match to that of SDSS J0805+4812 (top, solid line). All spectra are normalized at their $1.25 \mu\text{m}$ flux peaks, with the spectrum of 2MASS J1546–3325 scaled to match its relative flux compared to 2MASS J1507–1627 according to the M_K –spectral type relation of Burgasser (2007). [See the electronic edition of the Journal for a color version of this figure.]

Burgasser et al. 2002). The combined spectrum is an excellent match to that of SDSS J0805+4812 ($\chi^2 = 0.10$), reproducing the latter’s blue spectral energy distribution, enhanced 1.15 and $1.3 \mu\text{m}$ H_2O absorption bands, weak $2.3 \mu\text{m}$ CO absorption, and most notably the presence of weak CH_4 absorption at $1.6 \mu\text{m}$. Several combinations of midtype L dwarf and midtype T dwarf components produced similar excellent fits; in contrast, the single spectral templates were all poor matches ($\chi^2 > 1$). A mean of all binary spectral templates with $\chi^2 < 0.5$ (33 pairs) weighted by their inverse deviations yielded mean component types of $L4.6 \pm 0.7$ and $T4.9 \pm 0.6$. The inferred primary type is notably consistent with the optical classification of SDSS J0805+4812. This is an encouraging result, since L dwarfs are significantly brighter than T dwarfs at optical wavelengths and should thus dominate the combined light flux. The inferred secondary spectral type is significantly later, explaining both the presence (strong absorption) and weakness (lower relative flux) of the CH_4 feature at $1.6 \mu\text{m}$ in the composite spectrum of SDSS J0805+4812. Spectral types of L4.5 and T5 are hereafter adopted for the binary components of this system.

4. THE COMPONENTS OF SDSS J0805+4812

4.1. Estimated Physical Properties

Based on the excellent match of the spectrum of SDSS J0805+4812 to empirical binary templates composed of normal, single sources, it is compelling to conclude that unresolved binarity

³ For other examples of this technique, see the analyses of Burgasser et al. (2006, 2007a), Liu et al. (2006), Reid et al. (2006), Burgasser (2007), and Looper et al. (2007).

⁴ For an up-to-date list of known L and T dwarf binaries, see the VLM Binaries Archive maintained by N. Siegler at http://paperclip.as.arizona.edu/~nsiegler/VLM_binaries

⁵ Mauna Kea Observatory (MKO) photometric system (Simons & Tokunaga 2002; Tokunaga et al. 2002).

⁶ Here, $\chi^2 \equiv \sum_{\{\lambda\}} [f_{\lambda}(0805) - f_{\lambda}(SB)]^2 / f_{\lambda}(0805)$, where $f_{\lambda}(0805)$ is the spectrum of SDSS J0805+4812 and $f_{\lambda}(SB)$ is the spectrum of the synthesized binary over the set of wavelengths $\{\lambda\}$ as specified in the text.

TABLE 1
PREDICTED COMPONENT PARAMETERS FOR SDSS J0805+4812AB

Parameter	SDSS J0805+4812A	SDSS J0805+4812B	Difference
Spectral type	L4.5 \pm 0.7	T5 \pm 0.6	...
J^a	14.25 \pm 0.04	15.75 \pm 0.08	1.50 \pm 0.09
H^a	13.62 \pm 0.03	16.01 \pm 0.14	2.39 \pm 0.15
K^a	12.37 \pm 0.03	15.40 \pm 0.16	3.03 \pm 0.16
$\log L_{\text{bol}}/L_{\odot}^b$	-4.15 \pm 0.13	-4.93 \pm 0.13	0.88 \pm 0.16
Mass (M_{\odot}) at 1 Gyr ^c	0.066	0.036	0.55 ^d
Mass (M_{\odot}) at 5 Gyr ^c	0.078	0.069	0.88 ^d
T_{eff} (K) at 1 Gyr ^c	1830 \pm 90	1200 \pm 70	...
T_{eff} (K) at 5 Gyr ^c	1780 \pm 100	1100 \pm 70	...
Estimated d (pc)	14.5 \pm 2.1	14.8 \pm 2.5	-0.3 \pm 0.5

^a Synthetic magnitudes in the MKO system.

^b Luminosities based on the M_{bol} -spectral type relation of Burgasser (2007).

^c Based on the evolutionary models of Burrows et al. (2001) and the estimated luminosities.

^d Mass ratio (M_2/M_1).

provides the simplest explanation for the peculiarities of this source. Assuming this to be the case, it is possible to characterize the components of SDSS J0805+4812 in some detail. Component JHK magnitudes in the MKO system were determined from reported photometry of the source (Knapp et al. 2004) and integrating MKO filter profiles over the flux-calibrated binary template spectra. The best values, again using a weighted mean for all matches with $\chi^2 < 0.5$, are listed in Table 1. Comparison of the component magnitudes to absolute magnitude-spectral type relations from Burgasser (2007) yields distance estimates of 14.5 ± 2.1 and 14.8 ± 2.5 pc for the primary and secondary, respectively, where the uncertainties of the spectral types of the components and photometric magnitudes are explicitly included. It is of no surprise that these distance estimates are consistent, since the binary templates from which the component types are inferred are flux-calibrated using the same absolute magnitude scales. A mean distance of 14.6 ± 2.2 pc is estimated for this system.

The secondary is considerably fainter than the primary, particularly at K band, where $\Delta K = 3.03 \pm 0.16$ is deduced. This suggests a low system mass ratio ($q \equiv M_2/M_1$). Using the relative K -band flux and K -band bolometric corrections from Golimowski et al. (2004) and assuming $q \approx 10^{-0.15\Delta M_{\text{bol}}}$ (Burrows et al. 2001), $q = 0.48$ is inferred. This value is indeed smaller than the mass ratios of most very low mass binaries, 77% of which have $q \geq 0.8$ (Burgasser et al. 2007b). However, the approximation used here assumes that both components are brown dwarfs. The primary is of sufficiently early type that it may be an older hydrogen-burning low-mass star or massive brown dwarf. Using the evolutionary models of Burrows et al. (2001) and assuming component luminosities calculated from the M_{bol} -spectral type relation of Burgasser (2007),⁷ the estimated component masses and T_{eff} values for ages of 1 and 5 Gyr were computed and are listed in Table 1. If SDSS J0805+4812 is an older system, the mass ratio of the system increases toward unity. This is because the slightly less massive substellar secondary has had a much longer time to cool to T dwarf temperatures, while the primary has settled onto the main sequence. The strong age dependence on mass ratio estimates for low-mass stellar/substellar binaries is an important bias that is frequently overlooked.

4.2. Li I Detection and Age/Mass Constraints

From the previous discussion, it is clear that a robust characterization of the SDSS J0805+4812 components requires an

age determination for the system, which is generally difficult for individual field sources. Age constraints may be feasible in this case, however, as the inferred luminosities of its components straddle the Li I depletion line (Rebolo et al. 1992; Magazzú et al. 1993), as illustrated in Figure 3. The so-called binary lithium test pointed out by Liu & Leggett (2005) states that if lithium is present in the atmosphere of both components of the system, a maximum age may be inferred. Conversely, if lithium is absent, a minimum age may be inferred. The most interesting case is the absence of lithium in the primary spectrum but its presence in the secondary spectrum, which restricts the age of the system to a finite range.

The presence of lithium in the primary may be inferred from the 6708 Å Li I line in the system's composite spectrum. Optical data from Hawley et al. (2002) show no obvious feature at this wavelength, indicating lithium depletion in the primary and a

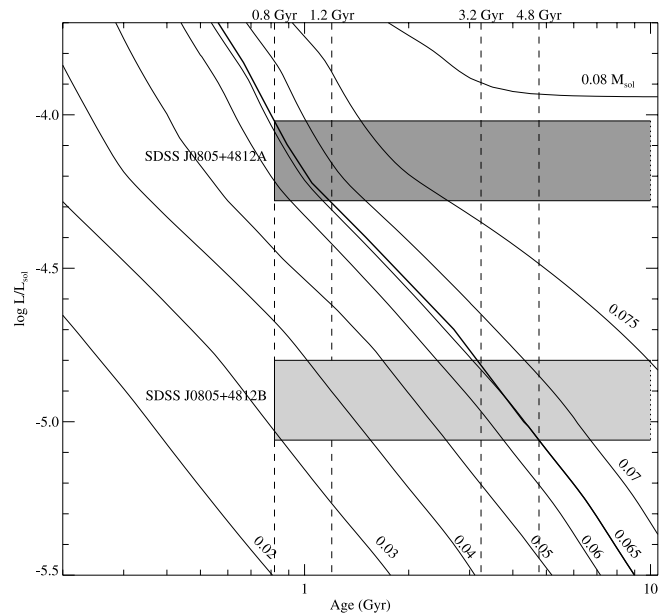


FIG. 3.—Limits on the masses and ages of the SDSS J0805+4812 components based on their estimated luminosities (gray regions) and evolutionary models from Burrows et al. (2001). Lines trace the evolutionary tracks for masses of 0.02–0.08 M_{\odot} . The lithium depletion boundary is indicated by the thickened line. Lower age limits assuming the absence of lithium in the atmospheres of the primary and secondary, and upper age limits assuming its presence, are indicated. The shaded regions are defined based on the absence of the 6708 Å Li I line in the combined light optical spectrum of SDSS J0805+4812 from Hawley et al. (2002).

⁷ Based on data from Golimowski et al. (2004).

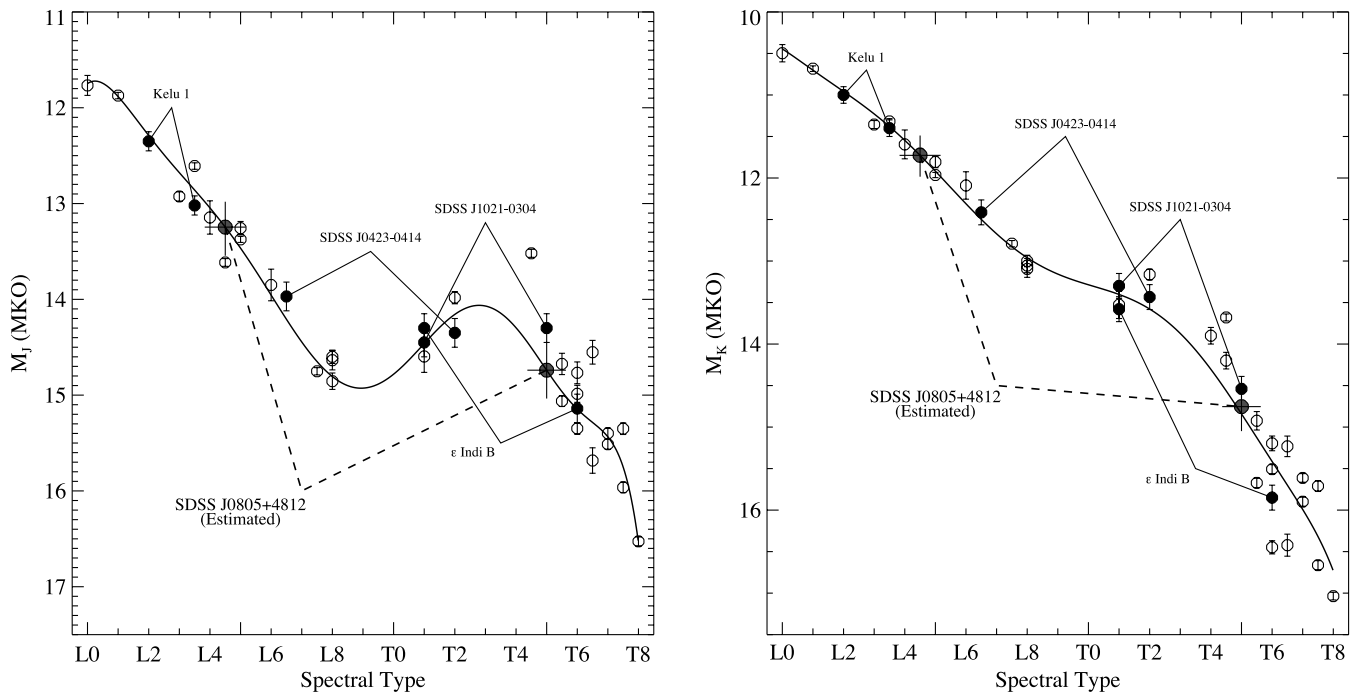


Fig. 4.— Absolute MKO J (left) and K (right) magnitudes for sources with absolute photometric errors less than 0.2 mag. Open circles indicate unresolved field objects, while filled circles indicate component magnitudes for the binaries Kelu 1AB, ϵ Indi Bab, SDSS J0423–0414AB, and SDSS J1021–0304AB. Photometric data are from Geballe et al. (2002), Leggett et al. (2002), Knapp et al. (2004), McCaughrean et al. (2004), Liu & Leggett (2005), and Burgasser et al. (2006); parallax data are from Perryman et al. (1997), Dahn et al. (2002), Tinney et al. (2003), and Vrba et al. (2004). The absolute magnitude–spectral type relations of Burgasser (2007) are delineated by thick lines. The predicted absolute magnitudes of the SDSS J0805+4812 components are indicated by large gray circles, assuming that the primary conforms to the absolute magnitude–spectral type relations. [See the electronic edition of the Journal for a color version of this figure.]

minimum age of 0.8 Gyr for the system based on the evolutionary models of Burrows et al. (2001) and the estimated component luminosities. However, the optical data for this faint source may have insufficient signal-to-noise ratio, and the absence of the Li I line requires confirmation. For the secondary, the 6708 Å Li I line is not expected to be seen even if this component is substellar, as atomic Li is expected to be depleted to LiCl below temperatures of ~ 1500 K (Lodders 1999). In this case the presence of lithium requires detection of the weak $15\ \mu\text{m}$ band of LiCl, which has yet to be detected in any T dwarf. Nevertheless, if LiCl could be detected in the spectrum of this component, the system’s age could be constrained to 1–5 Gyr. Future observational work, perhaps with the *James Webb Space Telescope*, may eventually provide the necessary observations to make this age determination.

4.3. SDSS J0805+4812 and the L/T Transition

As the inferred components of SDSS J0805+4812 appear to widely straddle the L/T transition, their relative magnitudes provide a good test of absolute magnitude–spectral type relations across this transition. Figure 4 displays M_J and M_K magnitudes for 28 L and T dwarfs with accurate parallax measurement ($\sigma_M \leq 0.2$ mag) and the eight components of the binaries Kelu 1AB (Liu & Leggett 2005), ϵ Indi Bab (McCaughrean et al. 2004), SDSSp J042348.57–041403.5AB (hereafter SDSS J0423–0414; Geballe et al. 2002; Burgasser et al. 2005) and SDSS J102109.69–030420.1AB (hereafter SDSS J1021–0304; Leggett et al. 2000; Burgasser et al. 2006). To place the components of SDSS J0805+4812 on this plot, the absolute magnitudes of the primary were set to those expected from the relations from Burgasser (2007), which are equivalent to results from other studies for midtype L dwarfs (e.g., Tinney et al. 2003; Knapp et al. 2004; Vrba et al. 2004; Liu et al. 2006). The absolute magnitudes of the secondary were then computed using the relative magnitudes listed in Table 1.

In both bands, there is excellent agreement between the secondary magnitudes and the absolute magnitude–spectral type relations shown. This is not surprising at K band, since the spectral templates used in the binary analysis were all flux-calibrated according to this relation. However, the agreement at J band is encouraging, particularly as the derived M_J for SDSS J0805+4812B, 14.7 ± 0.3 , is also consistent with absolute magnitudes for other T5–T5.5 sources. This magnitude is also equivalent to values for the latest-type L dwarfs and the T1–T5 components of the resolved binaries ϵ Indi Bab, SDSS J0423–0414, and SDSS J1021–0304, suggesting a “plateau” in the M_J –spectral type relation across the L/T transition, corresponding to a slight increase in surface fluxes at 1.05 and $1.25\ \mu\text{m}$ (Burgasser et al. 2006; Liu et al. 2006). However, a larger ~ 0.5 mag brightening from types L8 to T3 cannot yet be ruled out. It is increasingly clear that the brightest known T dwarf, 2MASS J05591914–1404488 (Burgasser et al. 2000), with $M_J = 13.52 \pm 0.04$ (Dahn et al. 2002; Leggett et al. 2002), is almost certainly a binary despite remaining unresolved in high angular resolution observations (Burgasser et al. 2003a; M. Liu 2007, private communication).

The estimated spectral types and photometric properties of the SDSS J0805+4812 components are unique in that they straddle the L/T transition more widely than other L dwarf/T dwarf binaries identified to date. However, it is important to remember that these parameters are predictions based on the binary spectral template analysis. Resolved photometry, radial velocity monitoring, and/or parallax measurements would provide unambiguous confirmation of these results.

5. A NEW TECHNIQUE FOR LOW-MASS MULTIPLICITY STUDIES

In this article, it has been demonstrated that the peculiar spectrum of the L4/L9.5 SDSS J0805+4812 can be sufficiently

explained as the combined light spectrum of an L4.5 plus T5 unresolved binary. This source joins a growing list of L/T transition binaries, many of which exhibit the same spectral peculiarities as SDSS J0805+4812 (blue near-infrared colors and the presence of 1.6 μm CH₄ absorption without the 2.2 μm band) and have been subsequently resolved through high-resolution imaging (Cruz et al. 2004; Burgasser et al. 2005, 2006; Liu et al. 2006; Reid et al. 2006). The similarity in the spectral peculiarities of these sources suggests that other binaries composed of L and T dwarf components could be readily identified and characterized through analysis of low-resolution, combined-light, near-infrared spectroscopy alone, as has been demonstrated here. This is a promising prospect, as traditional high-resolution imaging or spectroscopic techniques are limited by resolution and geometry restrictions, such that closely separated binaries and/or distant binary systems can be overlooked. This is particularly a concern for brown dwarf binaries, over 80% of which have projected separations less than 20 AU (Burgasser et al. 2007b). The use of combined light spectra in binary studies are not subject to resolution limitations, enabling the identification of binaries independent of separation. Furthermore, low-resolution near-infrared spectroscopy is far less resource-intensive than high-resolution imaging and spectroscopic techniques, which require the use of large telescopes and/or space-based platforms.

On the other hand, spectral peculiarities arising from binaries can be discerned only over a limited range of mass ratios (e.g., they will not generally be seen in equal-mass systems), may be readily apparent only in systems composed of L dwarf plus T dwarf components, and must be distinguished from spectral peculiarities arising from other effects such as metallicity, surface gravity, or condensate cloud structure. Hence, the phase space

in which unresolved binaries may be identified via low-resolution spectroscopy may be restricted in a nontrivial way, and its characterization is beyond the scope of this study. Nevertheless, the results presented here should make it clear that low-resolution near-infrared spectroscopic analysis provides a complementary approach to traditional high-resolution imaging and spectroscopic techniques in the identification and characterization of low-mass stellar and substellar binaries.

The author would like to thank telescope operator Dave Griep and instrument specialist John Rayner at IRTF for their assistance during the observations, and the anonymous referee for her/his helpful critique of the original manuscript. This publication makes use of data from the Two Micron All Sky Survey, which is a joint project of the University of Massachusetts and the Infrared Processing and Analysis Center and funded by the National Aeronautics and Space Administration and the National Science Foundation. The 2MASS data were obtained from the NASA/IPAC Infrared Science Archive, which is operated by the Jet Propulsion Laboratory, California Institute of Technology, under contract with the National Aeronautics and Space Administration. This research has benefitted from the M, L, and T dwarf compendium housed at <http://DwarfArchives.org> and maintained by Chris Gelino, Davy Kirkpatrick, and Adam Burgasser. The authors wish to recognize and acknowledge the very significant cultural role and reverence that the summit of Mauna Kea has always had within the indigenous Hawaiian community. We are most fortunate to have the opportunity to conduct observations from this mountain.

REFERENCES

- Ackerman, A. S., & Marley, M. S. 2001, *ApJ*, 556, 872
 Allard, F., Hauschildt, P. H., Alexander, D. R., Tamanai, A., & Schweitzer, A. 2001, *ApJ*, 556, 357
 Basri, G., & Reiners, A. 2006, *AJ*, 132, 663
 Bate, M. R., Bonnell, I. A., & Bromm, V. 2002, *MNRAS*, 332, L65
 Bouy, H., Moraux, E., Bouvier, J., Brandner, W., Martín E. L., Allard, F., Baraffe, I., & Fernández, M. 2006, *ApJ*, 637, 1056
 Burgasser, A. J. 2007, *ApJ*, 659, 655
 Burgasser, A. J., Kirkpatrick, J. D., Cruz, K. L., Reid, I. N., Leggett, S. K., Liebert, J., Burrows, A., & Brown, M. E. 2006, *ApJS*, 166, 585
 Burgasser, A. J., Kirkpatrick, J. D., Reid, I. N., Brown, M. E., Miskay, C. L., & Gizis, J. E. 2003a, *ApJ*, 586, 512
 Burgasser, A. J.,Looper, D. L., Kirkpatrick, J. D., & Swift, B. 2007a, *ApJ*, submitted
 Burgasser, A. J., Reid, I. N., Leggett, S. J., Kirkpatrick, J. D., Liebert, J., & Burrows, A. 2005, *ApJ*, 634, L177
 Burgasser, A. J., Reid, I. N., Siegler, N., Close, L. M., Allen, P., Lowrance, P. J., & Gizis, J. E. 2007b, in *Planets and Protostars V*, ed. B. Reipurth, D. Jewitt, & K. Keil (Tucson: Univ. Arizona Press), 427
 Burgasser, A. J., et al. 2000, *AJ*, 120, 1100
 ———. 2002, *ApJ*, 564, 421
 ———. 2003b, *ApJ*, 592, 1186
 Burrows, A., Hubbard, W. B., Lunine, J. I., & Liebert, J. 2001, *Rev. Mod. Phys.*, 73, 719
 Burrows, A., & Sharp, C. M. 1999, *ApJ*, 512, 843
 Burrows, A., Sudarsky, D., & Hubeny, I. 2006, *ApJ*, 640, 1063
 Chabrier, G., Baraffe, I., Allard, F., & Hauschildt, P. 2000, *ApJ*, 542, 464
 Chappelle, R. J., Pinfield, D. J., Steele, I. A., Dobbie, P. D., & Magazzú, A. 2005, *MNRAS*, 361, 1323
 Chiu, K., Fan, X., Leggett, S. K., Golimowski, D. A., Zheng, W., Geballe, T. R., Schneider, D. P., & Brinkmann, J. 2006, *AJ*, 131, 2722
 Cooper, C. S., Sudarsky, D., Milson, J. A., Lunine, J. I., & Burrows, A. 2003, *ApJ*, 586, 1320
 Cruz, K. L., Burgasser, A. J., Reid, I. N., & Liebert, J. 2004, *ApJ*, 604, L61
 Cruz, K. L., Reid, I. N., Liebert, J., Kirkpatrick, J. D., & Lowrance, P. J. 2003, *AJ*, 126, 2421
 Cruz, K. L., et al. 2007, *AJ*, 133, 439
 Cushing, M. C., Rayner, J. T., Davis, S. P., & Vacca, W. D. 2003, *ApJ*, 582, 1066
 Cushing, M. C., Vacca, W. D., & Rayner, J. T. 2004, *PASP*, 116, 362
 Dahn, C. C., et al. 2002, *AJ*, 124, 1170
 Folkes, S. L., Pinfield, D. J., Kendall, T. R., & Jones, H. R. A. 2007, *MNRAS*, 378, 901
 Geballe, T. R., et al. 2002, *ApJ*, 564, 466
 Golimowski, D. A., et al. 2004, *AJ*, 127, 3516
 Hawley, S. L., et al. 2002, *AJ*, 123, 3409
 Kirkpatrick, J. D. 2005, *ARA&A*, 43, 195
 Kirkpatrick, J. D., et al. 2000, *AJ*, 120, 447
 Knapp, G., et al. 2004, *AJ*, 127, 3553
 Leggett, S. K., Saumon, D., Marley, M. S., Geballe, T. R., Golimowski, D. A., Stephens, D., & Fan, X. 2007, *ApJ*, 655, 1079
 Leggett, S. K., et al. 2000, *ApJ*, 536, L35
 ———. 2002, *ApJ*, 564, 452
 Liu, M. C., & Leggett, S. K. 2005, *ApJ*, 634, 616
 Liu, M. C., Leggett, S. K., Golimowski, D. A., Chiu, K., Fan, X., Geballe, T. R., Schneider, D. P., & Brinkmann, J. 2006, *ApJ*, 647, 1393
 Lodders, K. 1999, *ApJ*, 519, 793
 Looper, D. L., Liu, M. C., Burgasser, A. J., Gelino, C. R., & Kirkpatrick, J. D. 2007, *ApJ*, in press
 Magazzú, A., Martín, E. L., & Rebolo, R. 1993, *ApJ*, 404, L17
 Marley, M. S., Seager, S., Saumon, D., Lodders, K., Ackerman, A. S., Freedman, R., & Fan, X. 2002, *ApJ*, 568, 335
 Maxted, P. F. L., & Jeffries, R. D. 2005, *MNRAS*, 362, L45
 McCaughrean, M. J., Close, L. M., Scholz, R.-D., Lenzen, R., Biller, B., Brandner, W., Hartung, M., & Lodieu, N. 2004, *A&A*, 413, 1029
 Perryman, M. A. C., et al. 1997, *A&A*, 323, L49
 Pinfield, D. J., Dobbie, P. D., Jameson, R. F., Steele, I. A., Jones, H. R. A., & Katsiyannis, A. C. 2003, *MNRAS*, 342, 1241
 Rayner, J. T., Toomey, D. W., Onaka, P. M., Denault, A. J., Stahlberger, W. E., Vacca, W. D., Cushing, M. C., & Wang, S. 2003, *PASP*, 115, 362
 Rebolo, R., Martín, E. L., & Magazzú, A. 1992, *ApJ*, 389, L83
 Reid, I. N., Kirkpatrick, J. D., Gizis, J. E., Dahn, C. C., Monet, D. G., Williams, R. J., Liebert, J., & Burgasser, A. J. 2000, *AJ*, 119, 369

- Reid, I. N., Lewitus, E., Cruz, K. L., & Burgasser, A. J. 2006, *ApJ*, 639, 1114
Simons, D. A., & Tokunaga, A. T. 2002, *PASP*, 114, 169
Sterzik, M. F., & Durisen, R. H. 2003, *A&A*, 400, 1031
Tinney, C. G., Burgasser, A. J., & Kirkpatrick, J. D. 2003, *AJ*, 126, 975
Tokunaga, A. T., Simons, D. A., & Vacca, W. D. 2002, *PASP*, 114, 180
Tsuji, T., Ohnaka, K., & Aoki, W. 1996, *A&A*, 305, L1
———. 1999, *ApJ*, 520, L119
Vacca, W. D., Cushing, M. C., & Rayner, J. T. 2003, *PASP*, 115, 389
Vrba, F. J., et al. 2004, *AJ*, 127, 2948
York, D. G., et al. 2000, *AJ*, 120, 1579